

## EXPERIMENTAL AND NUMERICAL STUDY OF THE TOOL-PART INTERACTION IN FLAT AND DOUBLE CURVATURE PARTS

Yüksel O.<sup>1</sup>, Çınar K.<sup>2</sup> and Ersoy N.<sup>1</sup>

<sup>1</sup>Department of Mechanical Engineering, , Boğaziçi University/ Bebek 34342 , Turkey

Email: onur.yuksel@boun.edu.tr, Web Page: <http://www.boun.edu.tr>

Email: nuri.ersoy@boun.edu.tr, Web Page: <http://www.boun.edu.tr>

<sup>2</sup>Department of Mechanical Engineering Namık Kemal University/, Corlu 59860, Turkey

Email: kcinar@nku.edu.tr, Web Page: <http://www.nku.edu.tr>

**Keywords:** Residual stress, process induced deformations, tool part interaction, deformation field, numerical model

### Abstract

A numerical model is developed to predict the process induced deformations of continuous fibre reinforced plastic plates which is made of AS4/8552 (Carbon fibre/epoxy) prepregs. In this way, Manufacturing costs can be reduced with elimination of trial and error approach. Sources of the process induced residual stress are clarified with the help of literature and implemented in 3D numerical model. In addition to the literature review to examine separate sources for residual stresses, an experimental measurement is conducted to observe tool part interaction which is quantified with strain gage which is embedded in prepreg. Numerical model is modified and verified with respect to overall deformation field of manufactured parts. Individual contribution of different mechanisms on overall deformation is discussed with the help of the numerical model. Moreover anisotropic friction between tool and the part is proposed to enhance the predictions of 3-D numerical model.

### 1. Introduction

Continuous fibre reinforced plastics are non-isotropic materials, composed of orthotropic plies in various configurations. Such configurations enable designers to produce structures in various stacking sequences with more rigidity and strength in the desired direction. On the other hand, this versatility of composite materials causes additional complexity for the manufacturing process. Due to the nature of the resin, composite manufacturing process should involve thermal processes. Different thermal properties of fibre and resin result in different thermomechanical behaviours in resin and fibre dominant directions. Non-isotropic thermal properties plus the simultaneous chemical shrinkage of the resin during the process cause process induced stresses. After curing, these stresses are locked in the structure as residual stresses. Residual stresses mostly induce out-of-plane deformations after the separation of the part from the mould. Therefore the prediction of the final deformation is crucial, however it should be calculated by a quantitative approach in order to obtain the final out-of-plane deformation field. This study presents a numerical model with three steps that predicts the out-of-plane deformation field according to the stacking sequence and geometry.

The reasons behind the process induced stresses can be classified with respect to the origin of the sources. Intrinsic sources depend on the material properties and extrinsic sources create residual stress due to the effect of the tool, bagging etc. which are related with the manufacturing techniques and geometry. On the other hand, sources for residual stress in composite materials can be separated with respect to their scale as micro and macro scale sources. Macro scale residual stress creates out-of-plane distortion in contrast with micro scale residual stress whose contribution on distortion is vanished due to self-equilibrating effect [1].

Residual stresses can be caused by cure shrinkage, thermal anisotropy, tool part interaction and other reasons. Cure shrinkage and thermal anisotropy lead out-of-plane deformations for curved parts because of the through thickness contraction at curved region. Both have similar effects on the final deformation. The only difference between them is the fact that the former occurs during curing of the resin and the latter occurs in the cooling period of the process cycle. Tool-part interaction which is another important cause of out-of-plane deformations has been examined by various researchers. Different thermal behaviour of tool and the composite part leads to shear stress between them. Stress formed in the tool side ply, transform through thickness direction with some decrease due to slipping motion between plies and shear compliance of the resin. That stress is locked in the part with curing and creates residual stress gradient through thickness which cause warpage for the flat parts when they are removed from the tool. Twigg *et al.* [2-4] and Gartska *et al.* [5] used strain gages in order to observe tool effect with different approaches. Different mechanisms can be the reason for residual stresses such as through thickness fibre volume fraction gradient and misaligned fibre orientation or fibre wrinkling [6]. In other words, process induced residual stresses and out-of-plane deformations can be caused by various reasons, however this study focuses on the main reasons which can be listed as thermal anisotropy, cure shrinkage and tool part interaction. For an extended review about residual stresses and related deformations, the review of Baran *et al.* [7] can be examined.

## 2. Material and Methods

In order to obtain a quantitative approach about residual stresses, a numerical model is developed in the light of the existing literature and previous studies. The numerical model, created in ABAQUS, is modified with respect to the resultant deformation field of experimental observations as a semi-inverse method. Contributions of the cure shrinkage and the thermal anisotropy are isolated with manipulations in numerical model. Difference between flat and double curvature tool are additionally helpful for observing these two mechanisms' contribution to the final deformation. Shear stresses between the tool and the part in the model is defined with respect to the observations coming from strain gage measurements. A comparative study regarding the experimental observations and numerical results is conducted.

### 2.1. Materials and Manufacturing

Flat plate and double curvature parts are cured on a steel tool made of IMPAX P20 hot work tool steel. CTE of tool material is  $12.6 \mu\text{m}/\text{m}^{\circ}\text{C}$ . Flat and doubly curved unidirectional  $[0]_4$  and crossply  $[0/90]_s$  parts of dimensions 300 mm x 300 mm are manufactured using an autoclave using carbon epoxy unidirectional prepregs, supplied by Hexcel Composites with AS4/8552 designation. One ply of uncured prepreg has 0.184 mm thickness and 57.4% nominal fibre volume fraction. Manufacturer's Recommended Cure Cycle The MRCC consists of a first ramp of  $2^{\circ}\text{C}/\text{min}$  up to  $120^{\circ}\text{C}$  and a first hold at  $120^{\circ}\text{C}$  for 60 min, a second ramp of  $2^{\circ}\text{C}/\text{min}$  up to  $180^{\circ}\text{C}$  and a second hold at  $180^{\circ}\text{C}$  for 120 min, and finally cooling to room temperature with a cooling rate of  $2^{\circ}\text{C}/\text{min}$ . A pressure of 0.7 MPa was applied from the beginning of the cycle.

### 2.2. Experimental Measurements

The deformation field of the manufactured parts are obtained by METRIS MCA II 7 axis 3-D laser scanner which is used for taking point clouds of the parts in their final geometries. These point clouds are compared with tool geometries in RAPIDFORM XOV software. Deformed shape of parts is virtually placed on tool. A colour map which visualizes vertical distance between the point cloud and tool surface is provided by the software.

Another part of the experimental work in this study is real-time strain measurement of the tool side ply. Pressure in the autoclave exerts normal force on prepreg through the cure cycle. At the same time, tool and composite in fibre direction have different coefficients of thermal expansion which creates the tensile stresses in the tool side fibres. Spot curing technique is used to measure that stress created by the tool. Without spot curing, prepreg is not convenient to attach strain gage on it, due to the viscous state of the resin. However, with spot curing technique strain gage is embedded to prepreg on a cured spot of 10 mm diameter. Resin is thermoset, so once it is cured with strain gage, it remains solid through cure cycle. Fibres are actual stress carriers therefore real time strain data can be measured with embedded strain gage. Fig. 1 demonstrates the set-up used for spot curing technique.

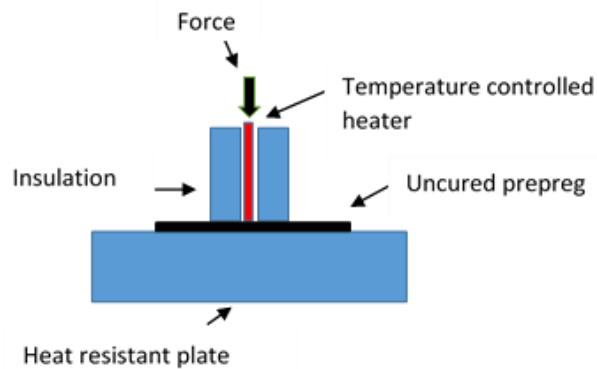


Figure 1. Spot curing setup.

### 2.3. Finite Element Model

A 3-D model with solid elements is implemented in ABAQUS to predict the out-of-plane deformations for flat and double curvature composite plates. Three steps are created to model three different states of resin as viscous, rubbery and glassy. Different material properties for different steps are assigned to the composite with user defined material (UMAT) code which propose constant properties for separate steps.

Physical properties and the chemical structure of resin varies during the cure cycle. Cross linking ratio increase with temperature rise and time, meanwhile the resin transforms from viscous to rubbery and then to glassy state. Ersoy *et al.* [8,9] claim that 30% and 70% degree of cure correspond to gelation and vitrification points at which the material properties are changed. In addition, degree of cure rises sharply in the middle portion of the second heating ramp. Transition from the rubbery to glassy state is occurred when the glass transition temperature is exceed by the autoclave temperature which occurs approximately 45 min after the beginning of second temperature holding period of cure cycle.

At the first step, resin is in viscous state which is ambiguous to define mechanical properties. Çınar *et al.* [10, 11, 12] worked on a parametric study in order to handle the effect of viscous mechanical properties on the final deformation field. They claim that resin dominated the mechanical properties of resin for viscous state is taken as 1/5<sup>th</sup> of the rubbery state mechanical properties. At the beginning of the second step, cross linking of the proceeds till the end of this step. Resin shrinkage during the curing is implemented into the model by negative coefficient of thermal expansion. Mechanical properties for the glassy state of the resin is used in the third step in which the residual stress developed is locked in part.

Due to differential thermal expansion behaviour of the tool and the composite part, relative displacement exists between tool and the part. Shear stress exerted by the friction is modelled with Coulomb friction model in which friction coefficient is constant up to a limiting shear stress. For the

first and the second step, limiting shear stress is 0.1 and 0.2 respectively. Experimentally measured stress of the tool side ply makes it possible to comment about the magnitude shear stress as explained in the Results section.

### 3. Results and Discussion

Firstly, tool part interaction measurement is presented. Then, comparison between manufactured part and numerical model which is modified with respect to the measured shear stress can be seen in the following sections.

#### 3.1. Tool-Part Interaction

After spot curing, uncured prepreg, in which strain gage is embedded, is tensile tested with INSTRON 8801. Thereby, strain gage measurement is calibrated to eliminate the misalignment, at the same time elastic modulus of prepreg is obtained, that is used for the derivation of shear stress, from the strain of tool side ply. Elastic modulus of the prepreg is measured as 126.125 GPa.

The following equation (Eq. 1) is used for the computation of shear strain.

$$\tau = \frac{\varepsilon t E}{L/2} \quad (1)$$

where  $L$  is the length,  $t$  is the thickness,  $E$  is the fibre direction elastic modulus of the prepreg and  $\tau$  and  $\varepsilon$  are shear stress and normal strain respectively. Strain values recorded during the process can be seen in Fig. 2. The strain signal is filtered to remove the noise (black line) as well as the change in temperature (green line) is shown in this figure. According to Eq. 1 shear stress is calculated as 0.172 MPa.

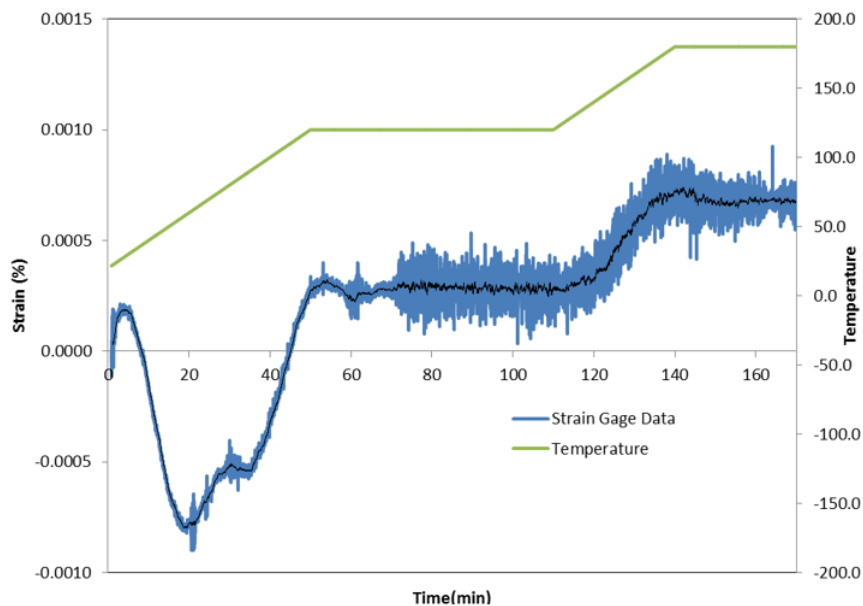


**Figure 1.** Raw data and moving average for real time strain data.

### 3. 2. Comparison of Experimental and Numerical Deformation Fields

The deformation field comparisons for flat part can be seen in Figs. 3-7. The field for unidirectional configuration  $[0]_4$  can be observed at Figs. 3 and 4. Then actual and predicted deformation fields for cross ply laminates  $[0/90]_s$  can be seen in Figs. 5 and 6.

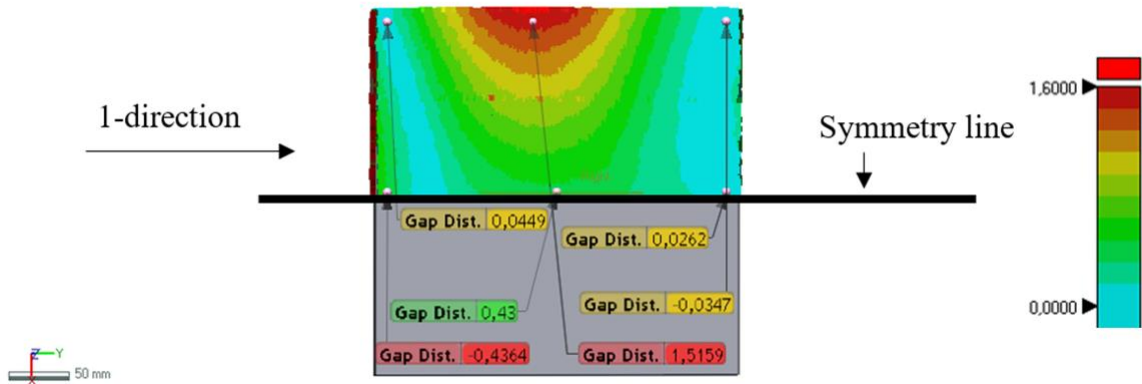


**Figure 3.** Measured distortion field for  $[0]_4$  flat part.

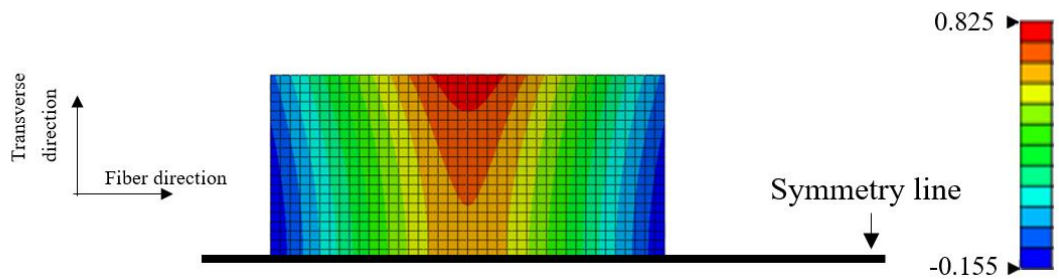


**Figure 4.** Finite element results for  $[0]_4$  flat parts.

For unidirectional flat parts, there is a concave down curvature along the fibre direction as can be estimated. Concave-up warpage in transverse direction is caused by the Poisson's effect. The form of the pre-given the tensile stresses induced in this direction due to tool-part interaction. Predicted deformation are very similar to the experimentally measured, however, there is a factor of 2 difference.

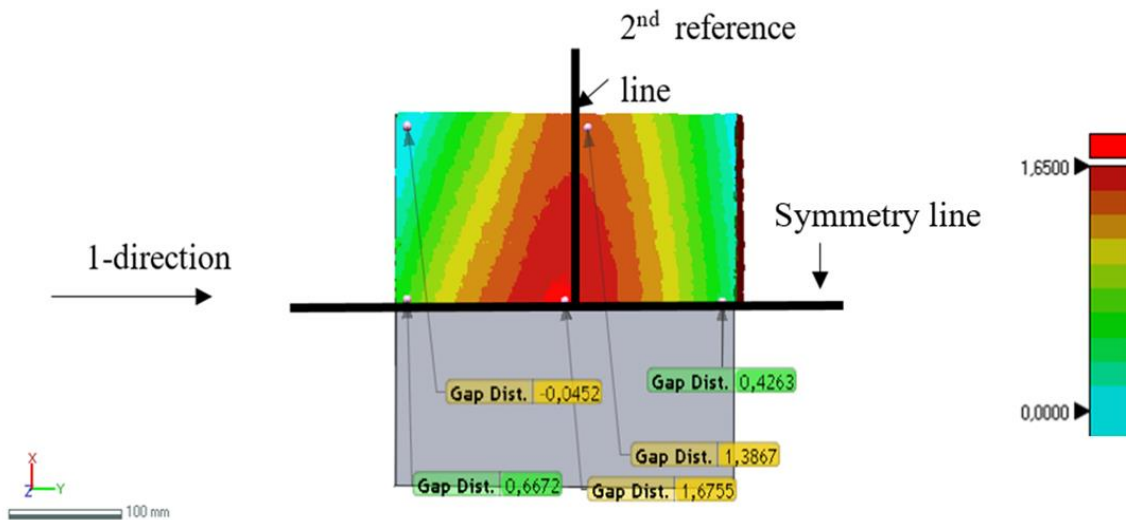


**Figure 5.** Measured distortion field for  $[0/90]_s$  flat part.

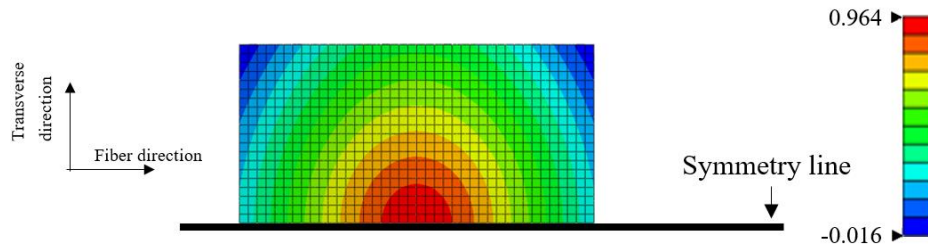


**Figure 6.** Finite element results for  $[0/90]_s$  flat part.

Predicted field for symmetric cross ply flat laminate is significantly different from the experimentally measured field. Probably, the friction coefficient in the transverse direction is lower due to the fact that fibers are perpendicular to the direction of relative motion between the tool and the ply. This is implemented into the model by using orthotropic frictional behavior between tool and part. The friction coefficient is kept at 0.3 in the fibre direction, and reduced by a factor of two in the transverse direction. Fig. 7 shows the deformation field handled with orthotropic frictional coefficient which is more close to the experimental field.

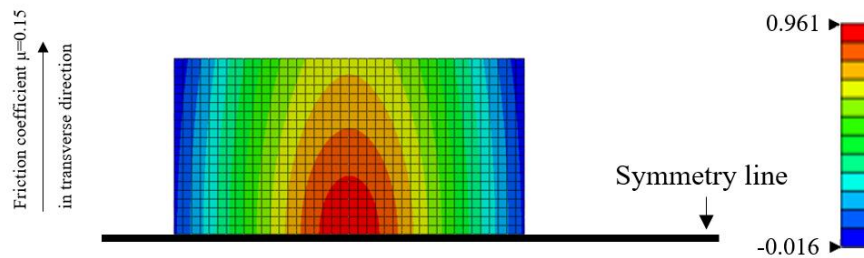


**Figure 7.** Modified distortion field with reduced transverse direction friction coefficient.

Comparison between numerical deformation field and experimentally observed deformation field for double curvature parts can be seen in Figs 8-11 below. The main difference of double curvature part is the contribution of thermal anisotropy and cure shrinkage effects on the overall deformation fields.

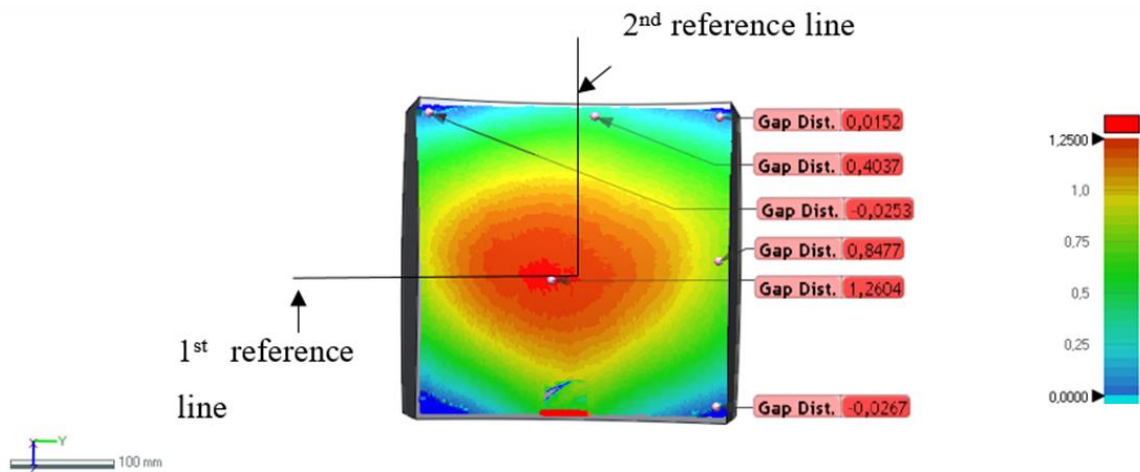


**Figure 8.** Measured distortion field for  $[0]_4$  double curvature part.

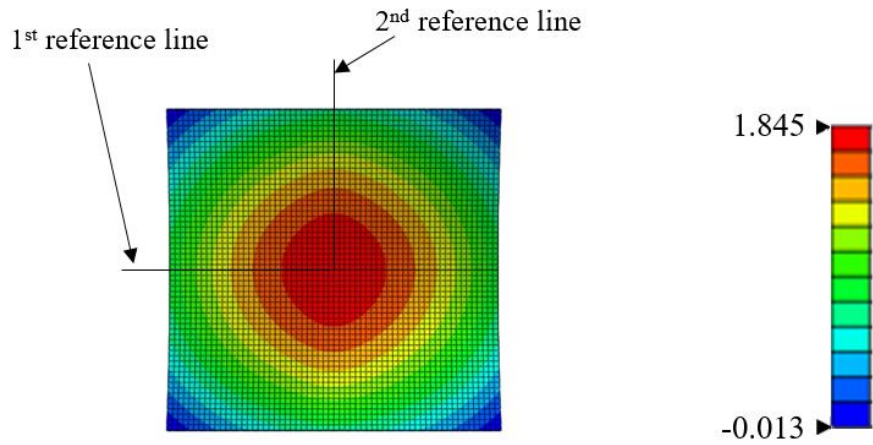


**Figure 9.** Finite element results for  $[0]_4$  double curvature part.

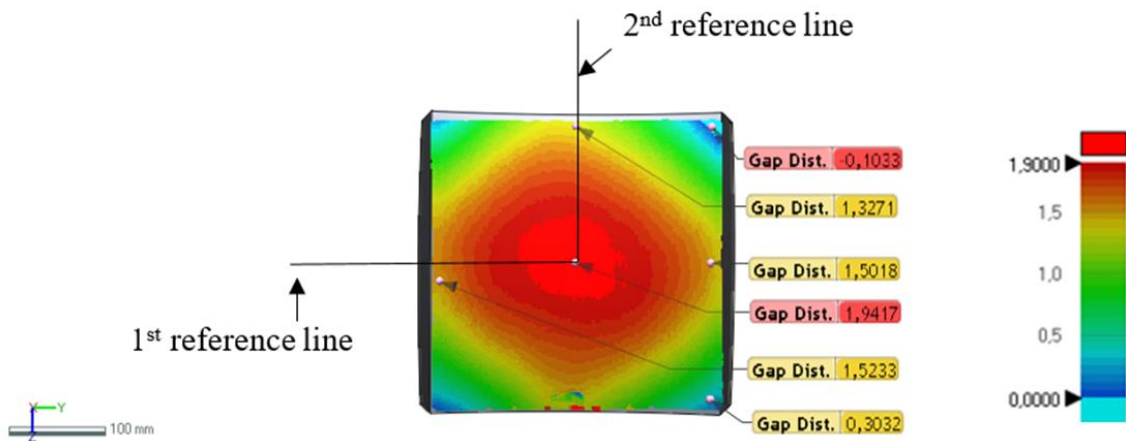


**Figure 10.** Measured distortion field for  $[0/90]_s$  double curvature part.

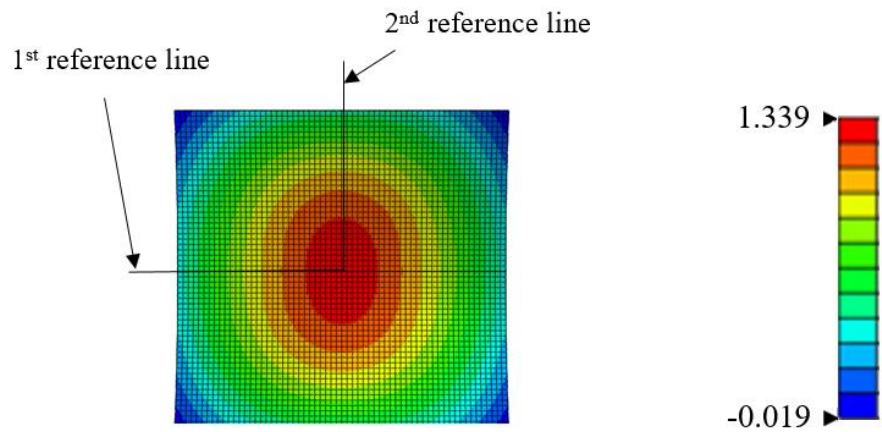


**Figure 11.** Finite element results for  $[0/90]_s$  double curvature part.

Figure 10 and Figure 11 show the observed and predicted deformation field for cross ply double curvature parts.

#### 4. Conclusion

In order to develop a numerical model which can predict the process induced residual stresses and out-of-plane deformations, a series of experiments are conducted. Composite parts with different stacking sequences and geometries are manufactured and their process induced distortion field is observed. Existing intuition about the process induced residual stresses is enhanced with quantitative approach provided by finite element method. Model developed in this study is validated by the strain gage measurements taken from the bottom ply which clarify the effect of tool-part interaction. As a semi inverse method, model is modified with respect to the observed deformation field and implement orthotropic friction coefficient is proposed as an improvement. It is found that numerical model predicts deformation fields reasonably well. As a future prospect, strain gage measurements should be reconducted for all plies and directions which can enlighten the shear stress transfer along the thickness direction.

#### References

- [1] Mazumdar, S.K., *Composites Manufacturing*, CRC Press, Florida, 2002.
- [2] Twigg, G., A. Poursartip, and G. Ferlund, "An Experimental Method for Quantifying Tool-part Shear Interaction during Composites Processing", *Composite Science and Technology*, Vol. 63, No. 13, pp. 1985-2002, 2003.
- [3] Twigg, G., A. Poursartip, and G. Ferlund, "Tool-part Interaction in Composite Processing. Part I: Experimental Investigation and Analytical Model", *Composite Part A*, Vol. 35, No. 1, pp. 121-133, 2004.
- [4] Twigg, G., A. Poursartip, and G. Ferlund, "Tool-part Interaction in Composite Processing. Part II: Numerical Modelling", *Composite Part A*, Vol. 35, No. 1, pp. 135-141, 2004.
- [5] Garstka, T., *Separation of Process Induced Distortions in Curved Composite Laminates*, Ph.D. Thesis, University of Bristol, 2005.
- [6] Çınar, K., N. Ersoy, "Effect of fibre wrinkling to the spring-in behaviour of L-shaped composite materials", *Composite Part A*, Vol. 69, No. 1, pp. 105-114, 2015.
- [7] Baran, I., K. Çınar, N. Ersoy, R. Akkerman, and J. H. Hattel, "A Review on the Mechanical Modeling of Composite Manufacturing Processes", *Archives of Computational Methods in Engineering*, pp 1-31, 2016.
- [8] Ersoy, N., T. Garstka, K. Potter, M.R. Wisnom, D. Porter, and G. Stringer, "Modelling of the Spring-in Phenomenon in Curved Parts Made of a Thermosetting Composite", *Composite Part A*, Vol. 41, No. 3, pp. 410-418, 2010.
- [9] Ersoy N., *et al.* "Development of the properties of a carbon fibre reinforced thermosetting composite through cure", *Composites: Part A*, Vol. 41, No. 3, pp. 401–9, 2010.
- [10] Çınar, K., *Process Modelling for Distortions in Manufacturing of Fibre Reinforced Composite Materials*, Ph.D. Thesis, Boğaziçi University, 2014.
- [11] Çınar, K., U.E. Öztürk, N. Ersoy, and M.R. Wisnom, "Modelling manufacturing deformations in corner sections made of composite materials", *Journal of Composite Materials*, Vol. 48, No. 7, pp. 799-813, 2014.
- [12] Çınar, K., N. Ersoy, "3D finite element model for predicting manufacturing distortions of composite parts", *Journal of Composite Materials*, Advance online publication, doi: 10.1177/0021998315625789, 2016.